Phys. Status Solidi B **254**, No. 8, 1600724 (2017) / **DOI** 10.1002/pssb.201600724

physica status solidi b
www.pss-b.com
basic solid state physics

High-temperature performance of non-polar (11–20) InGaN quantum dots grown by a quasi-two-temperature method

Tong Wang[1], Tim J. Puchtler[1], Tongtong Zhu[2], John C. Jarman[2], Rachel A. Oliver[2], and Robert A. Taylor[1]

[1] Department of Physics, University of Oxford, Parks Road, Oxford OX1 3PU, UK
[2] Department of Materials Science and Metallurgy, University of Cambridge, 27 Charles Babbage Road, Cambridge CB3 0FS, UK

Received 30 October 2016, revised 17 February 2017, accepted 22 May 2017
Published online 12 June 2017

Keywords growth, InGaN, microphotoluminescence, non-polar surfaces, quantum dots

* Corresponding author: e-mail tong.wang@physics.ox.ac.uk, Phone: +44 (0) 1865 272230, Fax: +44 (0) 1865 272400

The ORCID identification numbers for the authors of this article can be found under https://doi.org/10.1002/pssb.201600724.

Non-polar (11–20) *a*-plane InGaN quantum dots (QDs) are one of the strongest candidates to achieve on-chip applications of polarised single photon sources, which require a minimum operation temperature of ~200 K under thermoelectrically cooled conditions. In order to further improve the material quality and optical properties of *a*-plane InGaN QDs, a quasi-two-temperature (Q2T) method has been developed, producing much smoother underlying InGaN quantum well than the previous modified droplet epitaxy (MDE) method. In this work, we compare the emission features of QDs grown by these two methods at temperatures up to 200 K. Both fabrications methods are shown to be able to produce QDs emitting around the thermoelectric cooling barrier. The sample fabricated by the new Q2T method demonstrates more stable operation, with an order of magnitude higher intensity at 200 K comparing to the comparable QDs grown by MDE. A detailed discussion of the possible mechanisms that result in this advantage of slower thermal quenching is presented. The use of this alternative fabrication method hence promises more reliable operation at temperatures even higher than the thermoelectric cooling threshold, and facilitates the on-going development of high temperature polarised single photon sources based on *a*-plane InGaN QDs.

1 Introduction The realisation of quantum information processing [1], quantum metrology [2] and optical quantum computing [3] benefits from on-chip operation of single photon sources. The demonstrations of single photon emission in atoms [4], molecules [5], diamond nitrogen vacancy centres [6] and silicon carbide defect states [7] are fundamentally interesting, however, these systems offer limited potential for real-world applications in solid-state platforms. Quantum dots (QDs), on the other hand, can be fabricated using standard epitaxial growth techniques and integrated in a semiconductor system, and are thus in the vanguard of single photon research. A number of arsenide-based QD systems have achieved high purity, brightness, and indistinguishability [8–15], but are limited to operations under cryogenic conditions. Except for one single report for the observation of antibunching up to 135 K [16], arsenide QDs have not generally demonstrated operation beyond 100 K. The lowest temperature threshold for realistic operation in an integrated electronic platform is determined by thermoelectric cooling, a technique that makes use of the Peltier effect and has been widely adopted in various electronic products, such as charge-coupled devices (CCDs). Commercial Peltier-cooled electronic platforms are currently able to robustly and reproducibly maintain a stable temperature of ~200 K.

QDs based on III-nitrides offer much larger band offsets and exciton binding energies than the arsenide system, resulting in significantly stronger degrees of quantum

confinement and more stable operation at higher temperatures. A few nitride QD systems have achieved operation around and beyond 200 K [17–21], with the highest single photon emission temperature of 350 K demonstrated in a GaN/AlN dot-in-nanowire system [21]. However, although the use of nanowire-QDs offers further enhancement to the degree of quantum confinement and more stable operation at extreme temperatures, these structures are predicated on much more complex 3D growth routines, offering little prospect for the fabrication of electrically driven devices, and again undermining the original promise of on-chip applications.

To the best our knowledge, there have so far been only three reports of single photon generation at 200 K or higher in nitride systems with planar device structures [17, 18, 20], and of these only non-polar (11–20) *a*-plane InGaN QDs also demonstrate deterministic polarisation properties at 220 K [17]. The recent development of *a*-plane InGaN QDs have not only achieved significant reduction of the internal fields, faster radiative lifetimes [22, 23], Rabi oscillation [24], single photon generation [17] and polarised emission with a fixed polarisation axis [25], but also demonstrated most of these at temperatures beyond 200 K. As such, *a*-plane InGaN QDs are one of the strongest candidates to achieve the goals set forth in the beginning of this work.

In an attempt to further improve the properties of non-polar InGaN QDs, we here compare two different growth routines: the modified droplet epitaxy (MDE) method [23] and a new quasi-two-temperature (Q2T) method, adapted from an earlier two temperature (2T) method [22]. We note that the latter provides a way to create non-polar InGaN QDs lying on a relatively uniform quantum well (QW) layer, as opposed to the MDE method, in which disruption of the underlying quantum well (QW) layers is observed. We compare the emission properties of Q2T QDs with MDE QDs up to the Peltier cooling barrier of ∼200 K, and report more stable performances with Q2T structures at higher temperatures.

2 Method

2.1 Sample fabrication Both the Q2T and MDE routines are metal-organic vapour phase epitaxy methods, which are carried out in a 6×2 in. Thomas Swan close-coupled showerhead reactor on (11–20) *a*-plane GaN pseudo-substrates grown on *r*-plane sapphire [26], with precursors gases of trimethylgallium, trimethylindium and ammonia. At 690 °C and 300 Torr, a ∼16- (for Q2T) and 10-monolayer (for MDE) InGaN epilayer was grown. In the Q2T routine, this epilayer growth is immediately capped with ∼2 nm GaN layer at the same InGaN growth conditions. The temperature is then ramped and maintained at 860 °C, during which another cap of 8 nm GaN is grown, a process designed to produce better material quality. The growth conditions are otherwise similar to the 2T growth routine we have previously published [22], but in that case no low temperature cap was used. It should be noted that the thin cap is unlikely to fully cover the larger three dimensional nanostructures present in this sample prior to temperature ramping, so as in our previous approach these will be subjected uncapped to an anneal. In the MDE method, the sample is annealed in nitrogen atmosphere for period of 30 s, immediately after the growth of the InGaN epilayer, in order to induce the decomposition of InGaN QW and formation of metallic clusters. This process is then followed by a 10 nm capping layer grown at the same temperature, during which the metallic droplets are thought to re-react with ammonia to form QDs, and another 10 nm of GaN grown at 1050 °C using in H_2 atmosphere. Nanopillar structures (diameter ∼180 nm) have been post-processed in both samples for increased photon extraction efficiencies.

The key difference between the Q2T and MDE method is the use of a 30 s anneal process in N_2. As shown in Fig. 1

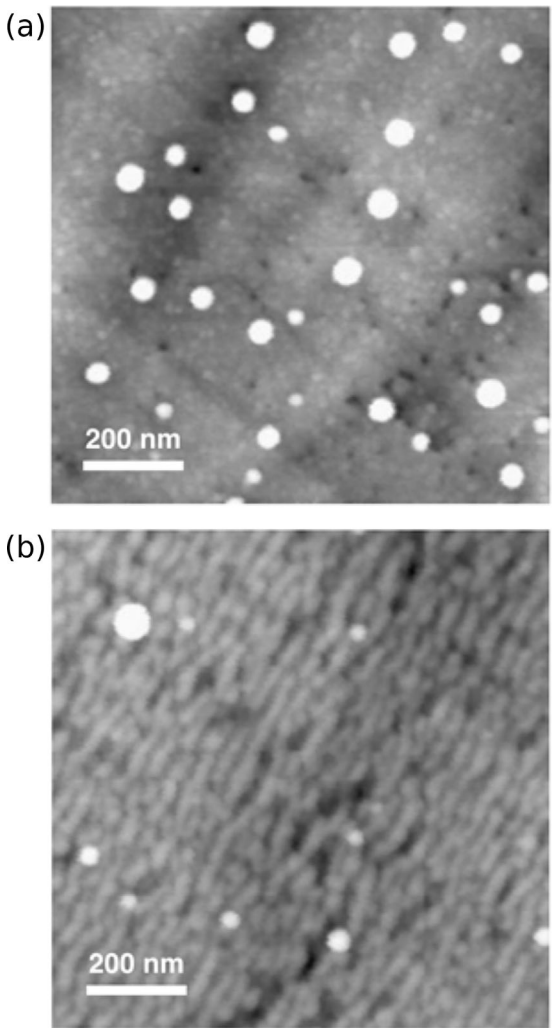

Figure 1 Atomic force microscope (AFM) images of (a) Q2T and (b) MDE samples before the growth of a GaN capping layer. In both cases, $h = 12$ nm. The bright spots are indicative of the formation of InGaN nanostructures and indium-rich metallic clusters, respectively. The degree of disruption to the underlying InGaN epilayer is much greater in the MDE sample than that in the Q2T sample.

(a), prior to capping, the morphology of the Q2T sample consists of isolated InGaN islands on a fairly smooth InGaN layer. On the other hand, in the MDE sample, we see not only metallic nanostructures but also a disrupted epilayer consisting of interconnected narrow fingers of InGaN, as shown in Fig. 1(b). Hence, based on the AFM data, we expect the QDs formed in the Q2T process to be found atop a much less disrupted underlying QW than is present in the MDE process.

2.2 Optical characterisation Microphotoluminescence (μ-PL) experiments have been performed on both Q2T and MDE samples in order to compare their optical properties and performances at high temperatures. An AttoDRY800 close-cycle cryostat is used to cool the sample to a stable temperature of 5 K. The regulators inside the cryostat are capable of increasing and stabilising the temperature with <15 mK accuracy up to 320 K. A 76 MHz repetition rate Ti:Sapphire laser generates 1 ps pulses at 800 nm, providing two-photon excitation. The resultant higher relative absorption cross-sections of QDs enhance dot-to-background ratios (DBRs) and improve the accuracy of optical characterisations [27]. The laser beam is spatially filtered and transmitted by a single-mode fibre, and collimated by the fibre output lens, before being directed to a 100× NIR objective with 0.5 N.A. Excitation pulses are focused to a ∼1 μm spot on the sample, whose movement is controlled by Attocube positioners. The PL from the sample is then collected by the same objective, and enters a 0.5 m Shamrock 500i spectrometer with a 100 μm slit and 1200 l/mm grating. The dispersed light is detected by a Peltier-cooled Andor iDus 420 CCD with a background noise of ∼3 counts/s, producing PL spectra with a ∼38 pm resolution.

3 Results A higher QD emission intensity is usually indicative of strong carrier confinement, and results in better temperature performance experimentally. As such, brighter QDs at 5 K should allow more accurate temperature analyses than ones with average emission intensity. Given the self-assembled nature of both Q2T and MDE QDs, it is difficult to find QDs with identical brightness, emission energy, DBR, and linewidth. However, in order to provide a comparison of their performances as precisely as possible, we chose two particular QDs in Fig. 2(a) and (b).

The peak intensities for the Q2T and MDE QD are both ∼900 counts/s at 5 K in our μ-PL setup, providing a similar starting point for the analysis of thermal quenching at higher temperatures. The linewidths are 2.59 ± 0.22 and 2.35 ± 0.20 meV for the Q2T and MDE QD respectively, which are reasonably similar within the errors, considering typical linewidths of *a*-plane InGaN QDs can vary between 300 μeV to 3 meV. Moreover, both QDs, emitting at 489 (Q2T) and 454 nm (MDE), are spectrally located at the higher energy ends of the underlying QW emission features, which are between 480–520 nm for the Q2T sample, and between 450–490 nm for the MDE case. The difference in

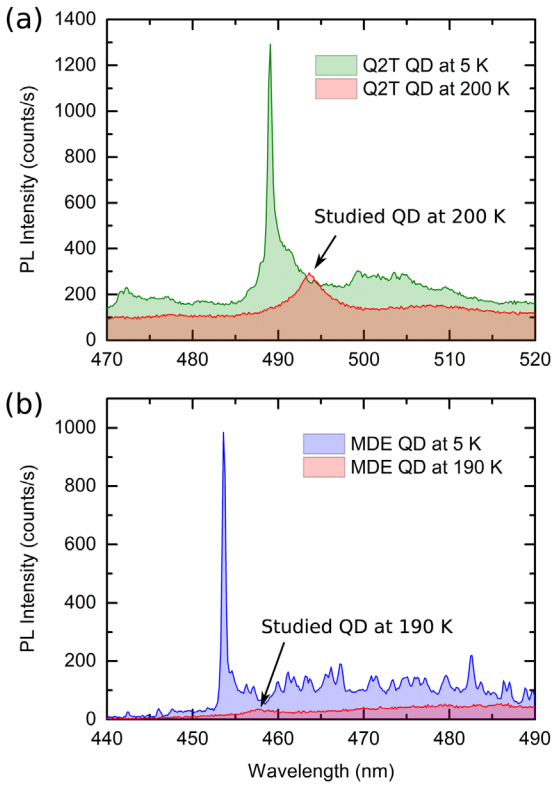

Figure 2 μ-PL spectra of (a) a Q2T and (b) an MDE QD with similar peak intensities at 5 K, emitting at 489 and 454 nm respectively. Also shown are the PL spectra of the same QDs at 200 K (Q2T) and 190 K (MDE), displayed on the same scale.

emission wavelength between the two samples occurs because more indium is lost during the anneal in nitrogen of the MDE sample than during the temperature ramp of the partially capped Q2T sample. Assuming similar QW emission mechanisms in the Q2T and MDE samples, the lower DBR in the Q2T sample is tentatively attributed to the greater area (within the same laser excitation spot) of underlying QW in the Q2T sample since in the MDE sample some of the QW is removed in the anneal step (cf. Fig. 1(b)). These features are demonstrated in Fig. 2(a) and (b), where the intensities of the QW background emission are different. The integrated count rates that arise from the underlying QW emission in the Q2T and MDE samples are 6.1×10^4 and 2.5×10^4 counts/s respectively.

The temperature of the samples is then gradually increased to ∼200 K, to investigate the optical characteristics of both Q2T and MDE QDs under temperatures reachable by Peltier cooling. The spectra at 200 K in Fig. 2 (a) and at 190 K in Fig. 2(b) thus confirm that *a*-plane InGaN QDs grown by either Q2T or MDE are able to emit at thermoelectrically regulated on-chip conditions. However, while the PL intensity of the Q2T QD is still very strong at 200 K, no QD signal can be detected beyond 190 K for the MDE QD. The normalised integrated intensities at 10 K intervals for both QDs are shown in Fig. 3, for more accurate analyses of their respective

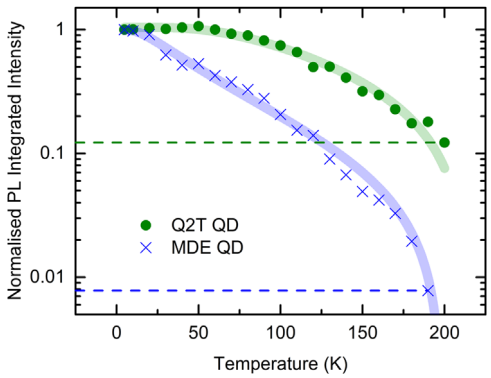

Figure 3 Temperature evolutions of integrated intensities of the Q2T and MDE QDs studied, normalised and displayed on a semi-log plot for easier observation of the behaviour at higher temperatures. The fitted curves are guides to the eye.

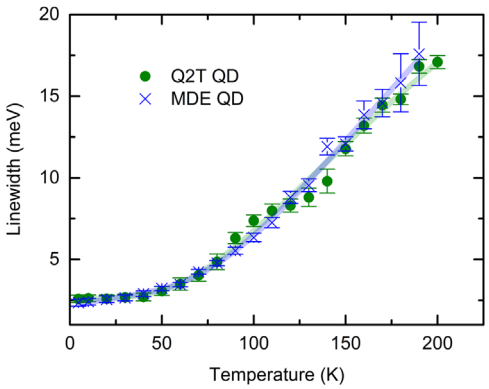

Figure 4 Temperature-dependent homogeneous linewidth broadening for the studied Q2T QD up to 200 K, and MDE QD up to 190 K. The fitted curves are phenomenological ones as basic descriptions to the data trends.

quenching behaviour. The intensity of the Q2T QD stayed mostly constant up to 60 K, and decreases very slowly till reaching ~12.2% of its original intensity at 5 K. Thus, the studied Q2T QD would be expected to emit at temperatures even higher than 200 K. On the other hand, the quenching of MDE QD intensity starts immediately after 10 K, and decreases at a much faster rate. At 190 K, the MDE QD intensity has already dropped to ~0.8% of that at 5 K. The order of magnitude stronger emission intensity of *a*-plane InGaN QDs grown by the Q2T method thus promises even better performance at higher temperatures. However, it is important to note that for other MDE QDs that are less strictly comparable, for example a QD with peak intensity of ~5000 counts/s at 5 K in Ref. [17], the much stronger confinement of the QD could result in similarly stable temperature performance as the studied Q2T QD, with an 11% integrated intensity at 220 K. In this case, the Q2T QD studied in this work has a similar temperature performance with only 20% of the initial brightness at 5 K, further demonstrating the promise of better temperature performance of Q2T QDs.

We attribute this difference in intensity quenching to three possible reasons. Firstly, due to the disrupted underlying InGaN epilayer, the energy profile of the QW in the proximity of the MDE QD would contain much greater fluctuations than in the Q2T case. The resulting potential minima act as potential carrier trapping sites. The excitons would hence possess higher probabilities to escape to those sites *via* processes such as tunnelling, providing a non-radiative pathway for carriers to leave the QD and thereby resulting in faster quenching of emission intensities. This is further supported by the evolution of the intensity DBRs. The DBR of the studied Q2T QD decreases from 2.25 (5 K) to 0.53 (200 K), while that of the MDE QD decreases from 9.01 (5 K) to 0.46 (190 K). The much faster reduction of DBR in the MDE case shows that carrier escape into surrounding QW is indeed an important contribution to QD intensity quenching.

Secondly, the slower escape of carriers could be attributed to deeper carrier confinement in the Q2T QDs, as may be indicated by the longer emission wavelength, which is due to a higher indium content. However, since carrier escape should be primarily into the surrounding QW, which also has a higher average indium content, this may not fully explain our observations.

Lastly, the interaction with phonons could also contribute differently to intensity quenching for both types of QDs. Hence, we compare the linewidth variations with temperature for both types of QDs, in order to gain insights into the degree of inelastic phonon scattering. The measured full-widths-at-half-maxima with their uncertainties from 5 to 200 K are presented in Fig. 4. Although the MDE QD starts off with a lower linewidth at 5 K, as mentioned in the previous text, the linewidth increased to 17.6 ± 1.9 meV at 190 K, which is similar to that of Q2T at 190 K (16.8 ± 0.4 meV). The exact broadening mechanisms are complex and not fully understood, but thermally assisted interaction with acoustic phonons has been considered as an important factor that contributes to the greater uncertainty of QD emission wavelength at higher temperatures [28, 29]. Unlike the contrast in integrated intensities (Fig. 3), the temperature evolutions of the linewidths are very similar to each other, and the linewidths at higher temperatures are identical within their measurement errors. This is not unexpected, since acoustic phonon coupling strength should be a property more related to the material itself and less to the microstructure. For instance, the published acoustic phonon scattering strengths of *c*-plane (0001) InGaN/GaN QDs are very similar to one another [28, 29], while that in *a*-plane InGaN/GaN QDs differs significantly from *c*-plane ones [30]. Hence, the main mechanism for intensity quenching should be the presence of non-radiative decay pathways in the underlying QWs for carrier escape from the QDs.

4 Conclusions The Q2T method is a MOVPE routine that does not involve any annealing process, and thus produces much less disrupted underlying InGaN epilayers, and thus fewer carrier escape pathways, than MDE. For this reason, the studied QD grown via the Q2T method not only emits more strongly at 200 K, but also has an integrated intensity more than an order of magnitude higher than a comparable MDE QD. However, due the self-assembled nature of our samples, there are significant variations in QD properties in energy, linewidth, brightness, and DBR. All of these could contribute to different temperature performances. Moreover, the stronger background QW emission in Q2T samples could pose challenges in obtaining higher DBRs and purer single photon emissions. More work, such as the use of a much thinner InGaN epilayer, needs to be done to reduce the emission from the QWs. Further development of *a*-plane Q2T QDs might lead to emission with much higher brightness and less background. These may then be better candidates for achieving even higher single photon emission temperatures above the thermoelectric cooling threshold. Nonetheless, this report shows that *a*-plane InGaN QDs fabricated with either growth method can achieve operation temperatures in the Peltier cooling regime, and are thus suitable for the development of on-chip single photon sources.

Acknowledgements This research was supported by the UK Engineering and Physical Sciences Research Council (EPSRC) Grants EP/M012379/1 and EP/M011682/1. T.W. is grateful for the award of the National Science Scholarship (NSS) as PhD funding by the Singapore Agency for Science, Technology and Research (A*STAR). R.A.O. is grateful to the Royal Academy of Engineering and the Leverhulme Trust for a Senior Research Fellowship.

Data access All data presented in Figs. 2–4 can be accessed free of charge online at https://doi.org/10.5287/bodleian:pvBNo9Mex

References

[1] C. Kurtsiefer, P. Zarda, M. Halder, H. Weinfurter, P. M. Gorman, P. R. Tapster, and J. G. Rarity, Quantum cryptography: A step towards global key distribution, Nature **419**, 450 (2002).
[2] V. Biovannetti, S. Lloyd, and L. Maccone, Quantum-enhanced measurements: Beating the standard quantum limit, Science **306**, 1330–1336 (2004).
[3] D. Loss and D. P. DiVincenzo, Quantum computation with quantum dots, Phys. Rev. A **57**, 120–126 (1998).
[4] H. J. Kimble, M. Dagenais, and L. Mandel, Photon antibunching in resonance fluorescence, Phys. Rev. Lett. **39**, 691–695 (1977).
[5] B. Lounis and W. E. Moerner, Single photons on demand from a single molecule at room temperature, Nature **407**, 491–493 (2000).
[6] N. Mizuochi, T. Makino, H. Kato, D. Takeuchi, M. Ogura, H. Okushi, M. Nothaft, P. Neumann, A. Gali, F. Jelezko, J. Wrachtrup, and S. Yamasaki, Electrically driven single-photon source at room temperature in diamond, Nature Photon. **6**, 299–303 (2012).
[7] S. Castelletto, B. C. Johnson, V. Ivády, N. Stavrias, T. Umeda, A. Gali, and T. Ohshima, A silicon carbide room-temperature single-photon source, Nature Mater. **13**, 151–156 (2013).
[8] N. Somaschi, V. Giesz, L. De Santis, J. C. Loredo, M. P. Almeida, G. Hornecker, S. L. Portalupi, T. Grange, C. Anton, J. Demory, C. Gomez, I. Sagnes, N. D. L. Kimura, A. Lemaitre, A. Auffeves, A. G. White, L. Lanco, and P. Senellart, Near-optimal single-photon sources in the solid state, Nature Photon. **10**, 340–345 (2016).
[9] X. Ding, Y. He, Z. C. Duan, N. Gregersen, M. C. Chen, S. Unsleber, S. Maier, C. Schneider, M. Kamp, S. Höfling, C. Y. Lu, and J. W. Pan, On-demand single photons with high extraction efficiency and near-unity indistinguishability from a resonantly driven quantum dot in a micropillar, Phys. Rev. Lett. **116**, 20401 (2016).
[10] Y. Wei, Y.-M. He, M. Chen, Y. Hu, Y. He, D. Wu, C. Schneider, M. Kamp, S. Höfling, C.-Y. Lu, and J.-W. Pan, Deterministic and robust generation of single photons on a chip with 99.5% indistinguishability using rapid adiabatic passage, Nano Lett. **14**, 6515 (2014).
[11] Y.-M. He, Y. He, Y.-J. Wei, D. Wu, M. Atatüre, C. Schneider, S. Höfling, M. Kamp, C.-Y. Lu, and J.-W. Pan, On-demand semiconductor single-photon source with near-unity indistinguishability, Nature Nanotechnol. **8**, 213–217 (2013).
[12] K. H. Madsen, S. Ates, J. Liu, A. Javadi, S. M. Albrecht, I. Yeo, S. Stobbe, and P. Lodahl, Efficient out-coupling of high-purity single photons from a coherent quantum dot in a photonic-crystal cavity, Phys. Rev. B **90**, 155303 (2014).
[13] M. E. Reimer, G. Bulgarini, N. Akopian, M. Hocevar, M. B. Bavinck, M. A. Verheijen, E. P. Bakkers, L. P. Kouwenhoven, and V. Zwiller, Bright single-photon sources in bottom-up tailored nanowires, Nature Commun. **3**, 737 (2012).
[14] O. Gazzano, S. Michaelis de Vasconcellos, C. Arnold, A. Nowak, E. Galopin, I. Sagnes, L. Lanco, A. Lemaître, and P. Senellart, Bright solid-state sources of indistinguishable single photons, Nature Commun. **4**, 1425 (2013).
[15] J. Claudon, J. Bleuse, N. S. Malik, M. Bazin, P. Jaffrennou, N. Gregersen, C. Sauvan, P. Lalanne, and J.-M. Gérard, A highly efficient single-photon source based on a quantum dot in a photonic nanowire, Nature Photon. **4**, 174–177 (2010).
[16] M. J. Stevens, R. H. Hadfield, R. E. Schwall, S. W. Nam, and R. P. Mirin, Quantum dot single photon sources studied with superconducting single photon detectors, IEEE J. Sel. Top. Quantum Electron. **12**, 1255–1268 (2006).
[17] T. Wang, T. J. Puchtler, T. Zhu, J. C. Jarman, L. P. Nuttall, R. A. Oliver, and R. A. Taylor, An ultrafast polarised single photon source at 220 K, arXiv:1610.00152, http://arxiv.org/abs/1610.00152 (2016).
[18] S. Kako, C. Santori, K. Hoshino, S. Götzinger, Y. Yamamoto, and Y. Arakawa, A gallium nitride single-photon source operating at 200 K, Nature Mater. **5**, 887–92 (2006).
[19] S. Deshpande, A. Das, and P. Bhattacharya, Blue single photon emission up to 200 K from an InGaN quantum dot in AlGaN nanowire, Appl. Phys. Lett. **102**, 161114 (2013).
[20] S. Deshpande, T. Frost, A. Hazari, and P. Bhattacharya, Electrically pumped single-photon emission at room temperature from a single InGaN/GaN quantum dot, Appl. Phys. Lett. **105**, 141109 (2014).

[21] M. J. Holmes, S. Kako, K. Choi, M. Arita, and Y. Arakawa, Single photons from a hot solid-state emitter at 350 K, ACS Photonics **3**, 543–546 (2016).

[22] J. T. Griffiths, T. Zhu, F. Oehler, R. M. Emery, W. Y. Fu, B. P. L. Reid, R. A. Taylor, M. J. Kappers, C. J. Humphreys, and R. A. Oliver, Growth of non-polar (11-20) InGaN quantum dots by metal organic vapour phase epitaxy using a two temperature method, APL Mater. **2**, 126101 (2014).

[23] T. Zhu, F. Oehler, B. P. L. Reid, R. M. Emery, R. A. Taylor, M. J. Kappers, and R. A. Oliver, Non-polar (11-20) InGaN quantum dots with short exciton lifetimes grown by metalorganic vapor phase epitaxy, Appl. Phys. Lett. **102**, 251905 (2013).

[24] B. P. L. Reid, C. Kocher, T. Zhu, F. Oehler, R. Emery, C. C. S. Chan, R. A. Oliver, and R. A. Taylor, Observations of Rabi oscillations in a non-polar InGaN quantum dot, Appl. Phys. Lett. **104**, 263108 (2014).

[25] T. Wang, T. J. Puchtler, S. K. Patra, T. Zhu, M. Ali, T. Badcock, T. Ding, R. A. Oliver, and R. A. Taylor, Experimental and theoretical analyses of strongly polarised photon emission from non-polar InGaN quantum dots, arXiv:1609.06885, https://arxiv.org/abs/1609.06885 (2016).

[26] F. Oehler, D. Sutherland, T. Zhu, R. Emery, T. J. Badcock, M. J. Kappers, C. J. Humphreys, P. Dawson, and R. A. Oliver, Evaluation of growth methods for the heteroepitaxy of non-polar (1120) GAN on sapphire by MOVPE, J. Cryst. Growth **408**, 32–41 (2014).

[27] A. F. Jarjour, A. M. Green, T. J. Parker, R. A. Taylor, R. A. Oliver, G. Andrew D. Briggs, M. J. Kappers, C. J. Humphreys, R. W. Martin, and I. M. Watson, Two-photon absorption from single InGaN/GaN quantum dots, Physica E, Low-Dimens. Syst. Nanostruct. **32**, 119–122 (2006).

[28] K. Sebald, H. Lohmeyer, J. Gutowski, T. Yamaguchi, and D. Hommel, Micro-photoluminescence studies of InGaN/GaN quantum dots up to 150 K, Phys. Status Solidi B **243**, 1661–1664 (2006).

[29] R. Seguin, S. Rodt, A. Strittmatter, L. Reißmann, T. Bartel, A. Hoffmann, D. Bimberg, E. Hahn, and D. Gerthsen, Multi-excitonic complexes in single InGaN quantum dots, Appl. Phys. Lett. **84**, 4023 (2004).

[30] B. P. L. Reid, T. Zhu, C. C. S. Chan, C. Kocher, F. Oehler, R. Emery, M. J. Kappers, R. A. Oliver, and R. A. Taylor, High temperature stability in non-polar (11-20) InGaN quantum dots: Exciton and biexciton dynamics, Phys. Status Solidi C **11**, 702–705 (2014).